Acta Crystallographica Section D
Biological Crystallography
ISSN 0907-4449

Structure of S35C flavodoxin mutant from *Desulfovibrio vulgaris* in the semiquinone state

R. Artali,[a]* N. Marchini,[a] F. Meneghetti,[a] D. Cavazzini,[b] A. Cassetta[c] and C. Sassone[d]

[a]Institute of Pharmaceutical Chemistry, University of Milano, Italy, [b]Department of Biochemistry and Molecular Biology, University of Parma, Italy, [c]Institute of Crystallography–CNR Trieste, Italy, and [d]Department of Human and Animal Biology, University of Torino, Italy

Correspondence e-mail: roberto.artali@tiscali.it

Received 21 October 2004
Accepted 14 January 2005

PDB Reference: S35C flavodoxin mutant, 1xt6, r1xt6sf.

The crystallographic structure of an engineered flavodoxin mutant from *Desulfovibrio vulgaris* has been analysed. Site-directed mutagenesis was used to substitute serine 35 with a cysteine to provide a possible covalent linkage. The crystal structure of the semiquinone form of this mutant is similar to the corresponding oxidation state of the wild-type flavodoxin. Analysis of the structural changes reveals the interaction between N(5)H of the flavin and the carbonyl O atom of Gly61 to be critical for modulation of the electrochemical properties of the protein.

1. Introduction

Flavodoxins are small members of the flavoproteins (molecular weight 14–23 kDa) which are highly stable soluble proteins that are easily isolated from a variety of microbial sources (Mayhew & Tollin, 1992). The presence of a noncovalently bound redox cofactor, riboflavin 5′-phosphate (FMN), confers electron-carrier properties in a variety of low-potential reactions. The prosthetic group can accept one or two electrons and consequently displays three oxidation states: oxidized (ox), the one-electron reduced semiquinone (sq) state and the two-electron reduced hydroquinone (hq) state (Ludwig & Luschinski, 1992), as shown in Fig. 1. The flavin sq is protonated at neutral pH (blue sq) and the pK_a of N(5)H is about 8.5; above this pH deprotonation occurs, producing the red anionic sq (Ehrenberg *et al.*, 1967); indeed, the pK_a of the hq state is 6.7 at N(1) (Dudley *et al.*, 1964; van Schagen & Muller, 1981).

Each redox state shows characteristic UV spectra, with a maximum peak of the oxidized state ranging between 374 and 444 nm depending on the environment. In particular, the binding of the flavin in the bacterial flavodoxins thermodynamically stabilizes the blue sq form (Ludwig & Luschinski, 1992; Mayhew & Tollin, 1992). A variety of FMN–protein interactions have been shown to play a role in tuning the midpoint potential of the cofactor, including short-range electrostatic interactions (Chang & Swenson, 1999; Hoover *et al.*, 1999), aromatic interactions (Lostao *et al.*, 2000; Zhou & Swenson, 1996) and hydrogen-bonding interactions at N(3) (Bradley & Swenson, 2001) and N(5) (Chang & Swenson, 1999; Hoover *et al.*, 1999; O'Farrell *et al.*, 1998). Much effort has been made towards producing high-quality X-ray crystal structures for several holoflavodoxins, often with the FMN in the three redox states. Comparisons of the three-dimensional structures of the oxidized form with at least one of the reduced states have been made for *Clostridium beijerinkii* MP (Smith *et al.*, 1977; Ludwig & Luschinski, 1992), *Megasphaera elsdenii* (Sharkey *et al.*, 1997; van Mierlo *et al.*, 1990), *Desulfovibrio vulgaris* (Watt *et al.*, 1991) and *Aspergillus nidulans* (Luschinsky *et al.*, 1992) flavodoxins. For these proteins, it has been assessed that the regulation of the redox properties of the flavin is influenced by protein conformational changes.

The short-chain flavodoxin from *D. vulgaris* has been used together with cytochromes c_{553} and P450$_{BM3}$ as a 'module' to generate multi-domain redox proteins for applications in sensor technology (Gilardi *et al.*, 2002; Sadeghi, Meharenna *et al.*, 2000; Sadeghi, Valetti *et al.*, 2000). The scaffold of the proteins is exploited to provide a controlled microenvironment capable of fine-tuning the redox properties of the resulting chimeras. The flavodoxin mutant S35C from *D. vulgaris* has been used as a 'building block' to construct artificial redox chains covalently linked *via* an engineered disulfide

bridge or by gene fusion. The advantages of using this protein lie in its small size, in the availability of the crystallographic structure, in the efficient recombinant expression system and in its capability to interact with electrode surfaces. In addition to these criteria, flavodoxins have been chosen for their low redox potentials, their homology to naturally occurring reductase domains of complex metabolic enzymes (Degtyarenko, 1995) and because of their well known electrochemical properties (Heering & Hagen, 1996). The S35C flavodoxin mutant was engineered with the aim of providing a link in the structure (the mutated cysteine) that could bind to the electrode surface through the formation of a disulfide bond. Determination of the crystal structure of the protein should allow the evaluation of the biochemical results in structural terms, which are needed for rational protein engineering and for the employment of computational methods for generating three-dimensional models of the possible complexes with other 'building blocks'.

This mutation site in flavodoxin has suitable solvent exposure, an efficient electronic coupling and complementary surface potentials with the redox partners. The mutation Ser35 *versus* Cys35 could permit the building of homodimers and heterodimers through the formation of a disulfide bridge, as already shown by the chimeras constructed using M23C and G51C cytochrome c_{553} mutants (Sadeghi, Meharenna *et al.*, 2000; Sadeghi, Valetti *et al.*, 2000). In addition, the redox potentials of the couples q/sq and sq/hq have been determined for wild-type flavodoxin at pH 7 and their values are −340 and −585mV *versus* Ag/AgCl, respectively, showing a pH-dependence of 51 mV per pH unit for the $E_{q/sq}$ potential (Astuti *et al.*, 2004). X-ray studies of q/sq flavodoxin wild-type forms (Watt *et al.*, 1991) have demonstrated that in the semiquinone state the reduction is accompanied by protonation of the cofactor N(5) nitrogen in agreement with the dependence of $E_{q/sq}$ on solution pH. The midpoint potential for the couple $E_{q/sq}$ of S35C has not yet been determined and X-ray investigation of the semireduced form could provide information about structural variation in relation to the midpoint potential evaluation. Here, we present the crystal structure at 1.8 Å resolution of the semireduced form of the S35C flavodoxin mutant monomer.

2. Experimental

2.1. Crystallization, data collection and data processing

Crystals of oxidized flavodoxin S35C mutant were grown using the sitting-drop vapour-diffusion method from a reservoir solution containing 3.2 *M* ammonium sulfate, 0.1 *M* Tris–HCl pH 7. Protein solution at a concentration ranging between 6 and 8 mg ml^{-1} was mixed in a 1:1 ratio with reservoir solution. Crystals grew at 298 K after about one week as well formed elongated yellow tetragonal bipyramids to dimensions of up to 0.2 × 0.3 × 0.7 mm. Crystals of the reduced form of the flavodoxin S35C mutant were obtained by dithionite reduction of the preformed crystals under aerobic conditions. S35C flavodoxin in its semiquinone form only was obtained by slowly adding reservoir solution containing 10 m*M* sodium dithionite to the crystals (Mayhew, 1978). The reduction was evidenced by the colour change of the crystals from yellow to dark blue after about 15 min and was checked by microspectrophotometric analysis: single-crystal polarized light spectra were recorded using a Zeiss UV–visible MPM800 microspectrophotometer by placing a single crystal in a quartz cell surrounded by its suspending medium (with or without dithionite) (Fig. 2). The crystal was oriented to collect spectra along the two main optical directions. We tried to reduce flavodoxin S35C crystals to the hydroquinone form under aerobic conditions by adjusting the buffer to pH 9 and then adding dithionite (Watt *et al.*, 1991; Vervoort *et al.*, 1994). However, under these experimental conditions we could only obtain FMN in the semiquinone form.

Prior to X-ray exposure, crystals were flash-frozen using the reservoir solution as a cryoprotectant and then placed on the goniometric head as they were very stable in the X-ray beam. The exposure time of the diffraction experiment was about 5 h. At the end of the diffraction experiment, the colour of the crystal was checked and remained blue, characteristic of the semireduced state of FMN.

A data set from 19.4 to 1.8 Å resolution was collected at 100 K from a single crystal at the Elettra synchrotron beamline (Trieste)

Table 1
Summary of X-ray data collection at XRD1, Elettra.

Values in parentheses refer to the highest resolution shell.

Space group	$P4_32_12$
Unit-cell parameters	
$a = b$ (Å)	51.08
c (Å)	138.42
Volume (Å^3)	354320.27
Resolution range (Å)	19.4–1.8 (1.91–1.8)
No. of measured reflections	218117
No. of unique reflections	17032 (14037)
Completeness (%)	99.6 (99.6)
R_{sym}	0.067 (0.211)
R_{merge} (%)	8.1 (83.7)
$I/\sigma(I)$	17.3 (2.3)
Multiplicity	11.1 (11.0)
No. of working reflections	14037 (1089)
No. of free reflections	1361 (109)
R_{work}	0.192 (0.206)
R_{free}	0.261 (0.282)
Estimated error in free R value	0.007 (0.027)
R.m.s.d. bond lengths (Å)	0.0063
R.m.s.d. bond angles (°)	4.30
No. of protein atoms	1102
No. of FMN atoms	31
No. of water molecules	176
Average B value for all atoms (Å^2)	18.98
Average B value for main chain	17.71
Average B value for side chain and waters	20.12
Average B for FMN atoms	15.54

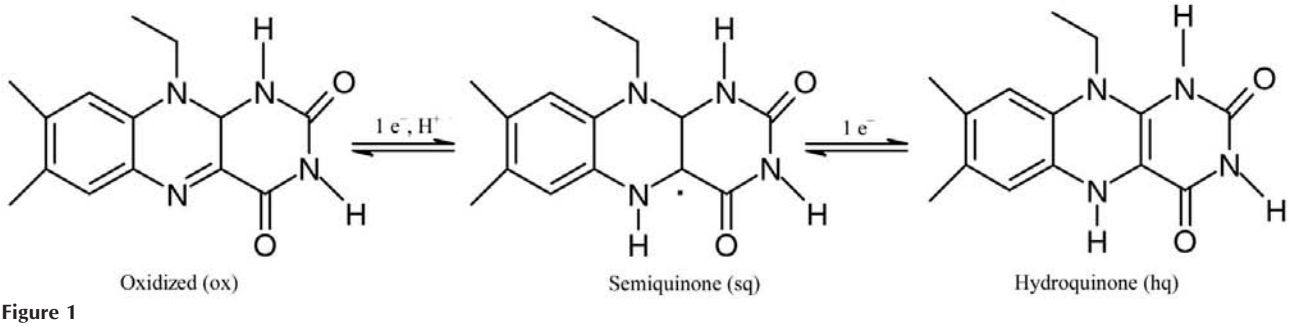

Figure 1
The isoalloxazine redox states.

with an X-ray wavelength of 1 Å using a MAR image-plate scanner. The program *MOSFLM* was used to elaborate each frame and *SORT* and *SCALA* (from the *CCP*4 suite; Collaborative Computational Project, Number 4, 1994) were used to index, process and scale the data.

The crystals belong to the same space group as wild-type flavodoxin. Other details of the data and model are presented in Table 1.

2.2. Refinement

The initial model was calculated using the coordinates of the oxidized S35C mutant flavodoxin (PDB code 1j9e; Artali *et al.*, 2002) and refined with *CNS* (Brünger *et al.*, 1998). The first refinement run yielded an overall R of 33.0% for all data with $I > 2\sigma(I)$. A randomly selected 10% of the data were set aside for cross-validation (Brünger, 1993). Manual rebuilding of the model and addition of the water molecules were performed using *XtalView* (McRee, 1993). An initial $2F_o - F_c$ map showed weak density for residues Glu42, Glu48, Asp76, Glu110, Asp127, Lys113 and Asp135. After simulated annealing and B-factor refinement, R and R_{free} fell to 29.1 and 32.9%, respectively, in the resolution range 19.4–1.8 Å. Subsequent modifications included adjustment of side chains and addition of water molecules guided by $F_o - F_c$ maps alternating with refinement. *XFIT* (McRee, 1993) was used to manually correct water peaks according to their distances from hydrogen-bonding partners. Solvent molecules with B values greater than 50 Å^2 and density lower than 1.5σ were deleted. Refinement converged at R = 25.5% and R_{free} = 32.1%. Analysis of the $2F_o - F_c$ map shows that residues Glu42, Glu48, Glu110, Lys113, Asp127 and Asp135 are disordered. The final model, containing 147 amino-acid residues, one FMN and 177 water molecules, yielded an R value of 19.20% and an R_{free} of 26.10%. The model was evaluated using *PROCHECK* (Laskowski *et al.*, 1993): all residues lie in allowed regions of the Ramachandran plot.

3. Results and discussion

The semi-reduced S35C flavodoxin contains the characteristic flavodoxin-like domain consisting of a central region of five parallel β-sheets flanked by two pairs of α-helices either side (Knauf *et al.*, 1996). As in all other flavodoxins, FMN primarily interacts with the apoprotein through hydrogen bonds and other non-bonded contacts (Ludwig & Luschinsky, 1992). The isoalloxazine moiety lies in an apolar environment, sandwiched between a tryptophan residue (Asp60, which flanks the inner face) and a tyrosine (Tyr98, which flanks the outer face) that is nearly coplanar with the tricyclic system. The ribityl side chain and the 5′-phosphate moiety of FMN also contribute to the cofactor binding through hydrogen-bond interactions with the polypeptide loop '8–13'. In particular, the 5′-phosphate moiety of FMN is not anchored by ion-pairing interactions but by hydrogen bonds with the phosphate-binding loop of the protein, which presents mainly serine and threonine residues. The majority of these interactions remain unchanged upon reduction and the structural changes of the S35C sq mutant are in the side-chain rearrangements in the '60-loop;'. The residues Asp62, Asp63 and Ser64 rotate away from the protein toward the solvent region, with shifts of about 3 Å closer to the flavin. The carbonyl oxygen of Gly61 moves from an orientation pointing away from the flavin ('O-down' conformation) to one pointing toward the isoalloxazine ring ('O-up' conformation), allowing the formation of a new hydrogen bond between the protein and the prosthetic group. This further interaction involving N(5)H of FMN and the backbone carbonyl O atom of Gly61 at a distance of 3.00 Å is comparable to that in wild-type sq (2.99 Å; Watt *et al.*, 1991) and is looser than in the other *D. vulgaris* flavodoxin D95A mutant (2.68 Å) in the sq state. It is interesting to

Table 2
R.m.s.d. values (Å) calculated on superimposing the structure of S35C mutant sq with the corresponding ox form and with wild-type (wt) sq.

Fitting was performed using the McLachlan algorithm (McLachlan, 1982) as implemented in the program *ProFiT*.

Superimposition	All atoms	Backbone	Side chain
S35C sq *versus* S35C ox	0.62	0.33	0.84
S35C sq *versus* S35C ox '60–64'	1.43	1.05	1.72
S35C sq *versus* wt sq	0.64	0.33	0.87
S35C sq *versus* wt sq '60–64'	0.81	0.43	1.07

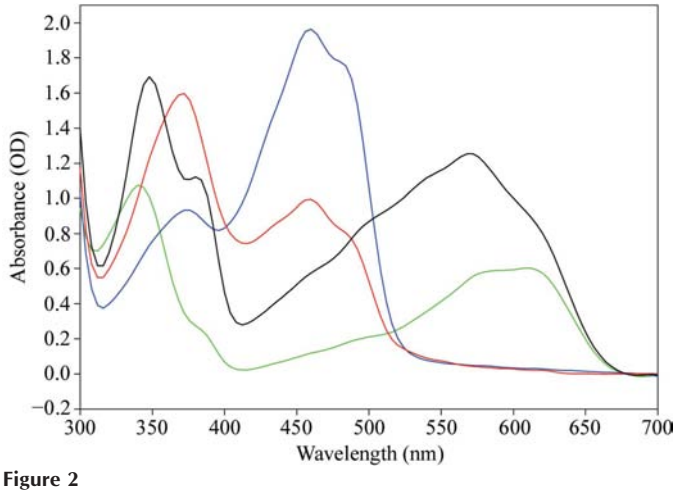

Figure 2
Polarized UV–Vis spectra of a single crystal of S35C flavodoxin mutant. The spectra were recorded on a S35C flavodoxin crystal with the electric vector of plane-polarized light parallel (oxidized, red line; semiquinone, black line) or perpendicular (oxidized, blue line; semiquinone, green line) to the crystallographic c axis.

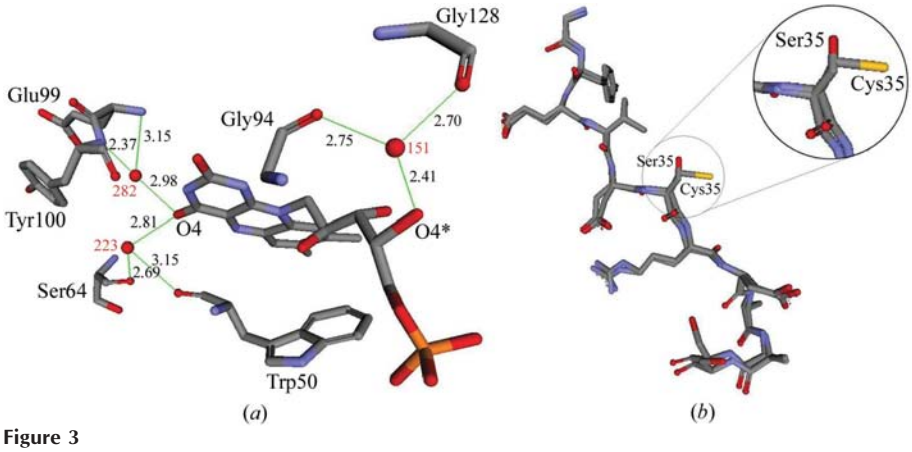

Figure 3
(*a*) Hydrogen-bonding interactions involving water molecules and FMN in the S35C mutant sq. (*b*) Superimposition of S35C sq and wild-type sq for the sequence 30–40; an enlargement of residue 35 is shown in the circle.

note that in the S35C mutant the structure modifications upon reduction are more similar to wild-type sq than the D95A mutant (McCarthy *et al.*, 2002), as in the latter the 60-loop reveals a larger movement away from the FMN. In wild-type sq Gly61 maintains the same conformational changes as in the hq state with small differences between the two forms, including a lengthening of the N(5)H···Gly61 O distance of 0.10 Å; we might thus expect for the S35C hq form the same trend as observed in wild-type sq upon further reduction. However, in the D95A mutant (McCarthy *et al.*, 2002) the crystal structures of the three oxidation forms have shown that the structural changes on reduction to the semiquinone are comparable with those observed in the wild type, while in the hq state, in contrast to the behaviour of the wild type in the same reduction state, unexpected conformational changes are determined in regions 61–64 and 96–99 that are responsible for the significant lengthening of the hydrogen bond by 0.35 Å between the Gly61 O and the N(5)H group of the isoalloxazine moiety of FMN.

The structural properties of the glycine residue and the role of the peptide flip have previously been investigated in several flavodoxin mutants (Chang & Swenson, 1999; Ludwig *et al.*, 1997). This 'O-up' conformation provides an additional flavin–protein interaction that is believed to contribute to the stabilization of the semiquinone form and plays a crucial role in controlling the midpoint potential of the couple ox/sq (O'Farrell *et al.*, 1998).

The structure of S35C sq has been compared with the mutant in the oxidized form (Artali *et al.*, 2002) and with the wild type in the reduced form (Watt *et al.*, 1991). The three structures have been superimposed and the r.m.s.d.s calculated. Table 2 reports the r.m.s.d.s of the sequence 60–64 involving Gly61.

The analysis of the hydrogen bonds between the prosthetic group and the mutant in the sq state reveals a similar pattern of interactions as in the oxidized state and in the wild type in the semireduced state. In S35C sq an interaction between Tyr100 and the O(4) of FMN mediated by a water molecule (W) is present with a distance Tyr100 N···W282 of 2.37 Å and W282···O(4) of 2.98 Å. The FMN is also connected to the protein by another solvent molecule (W223) bridging Ser64 O (2.69 Å) and Trp60 O (3.15 Å) and O(4) (2.81 Å), as shown in Fig. 3(*a*). In wild-type sq two water molecules interact with Ser64 O (2.69 Å) and Asp62 O (2.80 Å), respectively, while the corresponding distances from O(4) are 2.48 and 2.50 Å; a contact between them, not present in S35C sq, of 2.50 Å is also present.

Finally, the inspection of the mutation site shows that in the semireduced form, the Cys35 solvent exposure, calculated using the Connolly algorithm with a probe radius of 1.4 Å, is the same as in the oxidized state (Artali *et al.*, 2002). The orientation of the cysteine thiol group is the opposite of that of the serine hydroxyl group in the wild type (the torsion angles are −178.5 and −71.5° for Cys35 and Ser35, respectively), as shown in Fig. 3(*b*), in accordance with Nagano *et al.* (1999), who found cysteine residues to be preferentially located in hydrophobic clusters separated from serine and threonine.

We would like to thank Bracco Imaging for a grant to RA.

References

Artali, R., Bombieri, G., Meneghetti, F., Gilardi, G., Sadeghi, S. J., Cavazzini, D. & Rossi, G. L. (2002). *Acta Cryst.* D**58**, 1787–1792.

Astuti, Y., Topoglidis, E., Briscoe, P. B., Fantuzzi, A., Gilardi, G. & Durrant, J. R. (2004). *J. Am. Chem. Soc.* **126**, 8001–8009.

Bradley, L. H. & Swenson, R. P. (2001). *Biochemistry*, **40**, 8686–8695.

Brünger, A. T. (1993). *Acta Cryst.* D**49**, 24–36.

Brünger, A. T., Adams, P. D., Clore, G. M., DeLano, W. L., Gros, P., Grosse-Kunstleve, R. W., Jiang, J.-S., Kuszewski, J., Nilges, M., Pannu, N. S., Read, R. J., Rice, L. M., Simonson, T. & Warren, G. L., (1998). *Acta Cryst.* D**54**, 905.

Chang, F. C. & Swenson, R. P. (1999). *Biochemistry*, **38**, 7168–7176.

Collaborative Computational Project, Number 4 (1994). *Acta Cryst.* D**50**, 760–763.

Degtyarenko, K. N. (1995). *Protein Eng.* **8**, 737–747.

Dudley, K. H., Ehrenberg, A., Hemmerich, P. & Müller, F. (1964). *Helv. Chim. Acta*, **47**, 1354–1382.

Ehrenberg, A., Muller, F. & Hemmerich, P. (1967). *Eur. J. Biochem.* **2**, 286–293.

Gilardi, G., Meharenna, Y. T., Tsotsou, G. E., Sadeghi, S. J., Fairhead, M. & Giannini, S. (2002). *Biosens. Bioelectron.* **1–2**, 133–145.

Heering, H. A. & Hagen, W. R. (1996). *J. Electroanal. Chem.* **404**, 249–260.

Hoover, D. M., Drennan, C. L., Metzger, A. L., Osborne, C., Weber, C. H., Pattridge, K. A. & Ludwig, M. L. (1999). *J. Mol. Biol.* **294**, 725–743.

Knauf, M. A., Löhr, F., Mayhew, S. G. & Rüterjans, H. (1996). *Eur. J. Biochem.* **238**, 423–434.

Laskowski, R. A., MacArthur, M. W., Moss, D. S. & Thornton, J. M. (1993). *J. Appl. Cryst.* **26**, 283–291.

Lostao, A., El Harrous, M., Daoudi, F., Romero, A., Parody-Morreale, A. & Sancho, J. (2000). *J. Biol. Chem.* **275**, 9518–9526.

Ludwig, M. L. & Luschinsky, C. L. (1992). *Chemistry and Biochemistry of Flavoenzymes*, vol. 3, edited by F. Müller, pp. 427–466. Boca Raton, FL, USA: CRC Press.

Ludwig, M. L., Pattridge, K. A., Metzger, A. L., Dixon, M. M., Eren, M., Feng, Y. & Swenson, R. P. (1997). *Biochemistry*, **36**, 1259–1280.

Luschinsky, C. L., Dunham, W. R., Osborne, K. A., Pattridge, K. A. & Ludwig, M. L. (1992). *Flavins and Flavoproteins 1991*, edited by B. Curti, S. Ronchi & G. Zanetti, pp. 409–414. Berlin: Walter de Gruyter.

McCarthy, A. A., Walsh, M. A., Verma, C. S., O'Connell, D. P., Reinhold, M., Yalloway G. N., d'Arcy, D., Higgins, T. M., Voordouw, G. & Mayhew, S. G. (2002). *Biochemistry*, **41**, 10950–10962.

McLachlan, A. D. (1982). *Acta Cryst.* A**38**, 871–873.

McRee, D. (1993). *Practical Protein Crystallography*. San Diego: Academic Press.

Mayhew, S. G. (1978). *Eur. J. Biochem.* **85**, 535–547.

Mayhew, S. G. & Tollin, G. (1992). *Chemistry and Biochemistry of Flavoenzymes*, Vol. 3, edited by F. Müller, pp. 389–426. Boca Raton, FL, USA: CRC Press.

Mierlo, C. P. M. van, Lijnzaad, P., Veervoort, J., Müller, F., Berendsen, H. J. C. & De Vlieg, J. (1990). *Eur. J. Biochem.* **194**, 185–198.

Nagano, N., Ota, M. & Nishikawa, K. (1999). *FEBS Lett.* **458**, 69–71.

O'Farrell, P. A., Walsh, M. A., McCarthy, A. A., Higgins, T. M., Voordouw, G. & Mayhew, S. G. (1998). *Biochemistry*, **37**, 8405–8416.

Sadeghi, S. J., Meharenna, Y. T., Fantuzzi, A., Valetti, F. & Gilardi, G. (2000). *Faraday Discuss.* **116**, 135–153.

Sadeghi, S. J., Valetti, F., Cunha, C. A., Romao, M. J., Soares, C. M. & Gilardi, G. (2000). *J. Biol. Inorg. Chem.* **5**, 730–737.

Schagen, C. G. van & Muller, F. (1981). *Eur. J. Biochem.* **120**, 33–39.

Sharkey, C., Mayhew, S. G., Higgins, T. M. & Walsh, M. A. (1997). *Flavins and Flavoprotein 1996*, edited by K. K. J. Stevenson, V. Massey & C. H. Williams Jr, pp. 445–448. Calgary, Canada: University of Calgary Press.

Smith, W. W., Burnett, R. M., Darling, G. D. & Ludwig, M. L. (1977). *J. Mol. Biol.* **117**, 195–225.

Vervoort, J., Heering, D., Peelen, S. & van Berkel, W. (1994). *Methods Enzymol.* **243**, 185–203.

Watt, W., Tulinski, A., Swenson, R. P. & Watenpaugh, K. D. (1991). *J. Mol. Biol.* **218**, 195–208.

Zhou, Z. and Swenson, R. P. (1996). *Biochemistry*, **35**, 15980–15988.